Superconductivity in a narrow-band system with intersite electron pairing in two dimensions. II. Effects of nearest-neighbor exchange and correlated hopping

R. Micnas
Institute of Physics, A. Mickiewicz University, PL-60-769 Poznań, Poland

J. Ranninger
Centre National de la Recherche Scientifique, Centre de Recherches sur les Tres Basses Temperatures, Boîte Postale No. 166X, 38042 Grenoble, France

S. Robaszkiewicz*
Institut Laue-Langevin, Boîte Postale No. 166X, 38042 Grenoble, France
(Received 10 January 1989)

Our previous mean-field study concerning superconducting pairings in the extended Hubbard model with on-site repulsive and intersite attractive interaction and arbitrary electron density is extended to include the effects of nearest-neighbor exchange (J) and correlated hopping (K) interaction. Detailed numerical analysis of s-, p-, and d-wave pairing solutions is performed for the two-dimensional square lattice with nearest- (t) and next-nearest- (t_2) neighbor hopping, and the resulting mutual stability phase diagrams are given as a function of band filling and the interaction parameters. Antiferromagnetic exchange can enhance both the d-wave and the extended s-wave pairing. If it prevails over the repulsive intersite density-density interaction, such a term can be a leading mechanism for superconductivity. However, its effects strongly depend on the band filling and the t_2/t ratio, giving in particular for $t_2=0$ s-wave (d-wave) pairing as most favorable in the low (high) density limit, but increasing t_2 can even reverse this tendency. The correlated hopping term which breaks the electron-hole symmetry affects s-wave pairing mostly. A condensation transition (phase separation), possible in the presence of the attractive density-density interaction, is also analyzed within the random-phase approximation, and stability conditions of such an electron droplet phase with respect to other types of ordering are determined as a function of the band filling for the two-dimensional square lattice.

I. INTRODUCTION

In a recent paper[1] we studied a simple model of narrow-band materials with local attractive interaction of the following form:

$$H=\sum_{i,j,\sigma}(t_{ij}-\mu\delta_{ij})c_{i\sigma}^{\dagger}c_{j\sigma}+U\sum_i n_{i\uparrow}n_{i\downarrow}+\frac{1}{2}\sum_{i,j,\sigma,\sigma'}W_{ij}n_{i\sigma}n_{j\sigma'}, \tag{1.1}$$

where t_{ij} denotes the transfer integral, μ the chemical potential, U is the on-site Coulomb interaction, W_{ij} is the intersite interaction and $n_{i\sigma}=c_{i\sigma}^{\dagger}c_{i\sigma}$. The number of electrons per lattice site is given by

$$n=\frac{1}{N}\sum_{i,\sigma}\langle n_{i\sigma}\rangle . \tag{1.2}$$

This simple extended Hubbard model can be taken as a prototype to study the real-space pairing, either on-site ($U<0$) or intersite ($W<0$). The parameters of (1.1) are renormalized from their bare values, and the Hamiltonian (1.1) can be considered as rather general, resulting from the coupling of narrow-band electrons to the bosonic field, such as phonons, excitons, or plasmons. The induced attractive potential competes with the Coulomb repulsion and can give rise to a local attractive interaction. Such a nonretarded static, short-range attraction can also be of purely electronic origin due to, for example, strong polarizability of anions.

In Ref. 1 we considered the case $U>0$ and $W<0$, which is the simplest model to account for magnetism and intersite superconducting pairing. The term mainly responsible for the intersite pairing was the effective-nearest-neighbor (density-density) attraction $W_{ij}<0$.

In general, there are two other intersite interaction terms which are not included in (1.1) and which can be of importance in real narrow-band systems. They are given by

$$H_1=\sum_{i,j}J_{ij}\boldsymbol{\sigma}_i\cdot\boldsymbol{\sigma}_j+\frac{1}{2}\sum_{i,j,\sigma}K_{ij}n_{i\sigma}(c_{i-\sigma}^{\dagger}c_{j-\sigma}+\text{H.c.}), \tag{1.3}$$

where $\sigma_i^{\dagger}=c_{i\uparrow}^{\dagger}c_{i\downarrow}$, $\sigma_i^z=\frac{1}{2}(n_{i\uparrow}-n_{i\downarrow})$.

The main purpose of this work is to study the effects of just these terms on the superconductivity of a system with intersite pairing and to point out new features which can be introduced into the model (1.1) by these couplings. We shall also report further results for the model (1.1) concerning the problem of the electron droplet formation (phase separation) and of the mutual stability of superconducting and droplet phases.

Formally, J_{ij} and K_{ij} are the off-diagonal terms of the Coulomb interaction $V(\mathbf{r}-\mathbf{r}')$:[2,3]

$$J_{ij}=(ii\,|\,V(r)\,|\,jj),\quad K_{ij}=(ii\,|\,V(r)\,|\,ij).$$

These terms, involving bond charge density result from the fact that due to translational invariance, the electron density operator is not diagonal in a Wannier representation. The estimations of Hubbard,[2] Kivelson *et al.*,[4] Baeriswyl *et al.*,[5] and Gammel and co-workers[6,7] show that such terms can be of importance in narrow-band materi-

als. J_{ij} is the effective direct superexchange (potential exchange).[8] Both J_{ij} and K_{ij} can be renormalized by several factors, e.g., they can contain contributions from the electron-phonon coupling.[9-11]

As in Ref. 1, our study is concerned mainly with a two-dimensional (2D) square lattice employing the broken-symmetry Hartree-Fock scheme and considering the case of arbitrary electron density. Recently, some authors considered the exchange interaction terms as a possible mechanism for high-T_c superconductivity.[12-15] We think that the results of the present paper will provide deeper understanding of this problem also.

II. MEAN-FIELD THEORY

Our mean-field approach for the Hamiltonian $H+H_1$ follows exactly that presented in Ref. 1; therefore, here we shall only give the final basic equations for the particular types of pairings, restricting ourselves to the case of nearest-neighbor interactions.

A. Singlet superconducting phases

The gap equation for the singlet pairing is given by

$$\Delta_{\mathbf{k}}=\frac{1}{N}\sum_{\mathbf{q}}V^{s}_{\mathbf{k},\mathbf{q}}\langle c_{-\mathbf{q}\downarrow}c_{\mathbf{q}\uparrow}\rangle=\frac{1}{N}\sum_{\mathbf{q}}V^{s}_{\mathbf{k},\mathbf{q}}\Delta_{\mathbf{q}}F_{\mathbf{q}}\,, \tag{2.1}$$

where

$$V^{s}_{\mathbf{k},\mathbf{q}}=-U-W_{\mathbf{k}-\mathbf{q}}+\tfrac{3}{2}J_{\mathbf{k}-\mathbf{q}}-(K_{\mathbf{k}}+K_{\mathbf{q}})\,, \tag{2.2}$$

$$F_{\mathbf{q}}=(2E_{\mathbf{q}})^{-1}\tanh(\beta E_{\mathbf{q}}/2)\,, \tag{2.3}$$

$$E_{\mathbf{q}}=\sqrt{\bar{\varepsilon}_{\mathbf{q}}^{2}+|\Delta_{\mathbf{q}}|^{2}}\,. \tag{2.4}$$

$$\bar{\varepsilon}_{\mathbf{q}}=\varepsilon_{\mathbf{q}}-pW\gamma_{\mathbf{q}}/\gamma_0+K\gamma_{\mathbf{q}}n/2-\tfrac{3}{2}pJ\gamma_{\mathbf{q}}/\gamma_0-\bar{\mu}\,,$$

$$\varepsilon_{\mathbf{q}}=-\sum_{j}t_{ij}\exp[i\mathbf{q}\cdot(\mathbf{R}_i-\mathbf{R}_j)]\,,$$

$$\bar{\mu}=\mu-n\left(\frac{U}{2}+W_0\right)-pK\,, \tag{2.5}$$

$$\beta=(k_BT)^{-1}\,.$$

$$\begin{pmatrix} 1+U\Phi_1+K\Phi_2 & U\Phi_2+K\Phi_\gamma \\ \tfrac{1}{4}(W-\tfrac{3}{2}J)\Phi_2+K\Phi_1 & 1+\tfrac{1}{4}(W-\tfrac{3}{2}J)\Phi_\gamma+K\Phi_2 \end{pmatrix}\begin{pmatrix}\Delta_0\\ \Delta_\gamma\end{pmatrix}=0\,, \tag{2.11}$$

with p and μ given as Eqs. (2.6)-(2.7) for $\Delta_{\mathbf{q}}\to 0$. In Eq. (2.11)

$$\Phi_1=\frac{1}{N}\sum_{\mathbf{q}}F_{\mathbf{q}}(T_c)\,,$$

$$\Phi_2=\frac{1}{N}\sum_{\mathbf{q}}\gamma_{\mathbf{q}}F_{\mathbf{q}}(T_c)\,, \tag{2.12}$$

$$\Phi_\gamma=\frac{1}{N}\sum_{\mathbf{q}}\gamma_{\mathbf{q}}^{2}F_{\mathbf{q}}(T_c)\,,$$

and

$$F_{\mathbf{q}}(T_c)=(2\bar{\varepsilon}_{\mathbf{q}})^{-1}\tanh(\beta_c\bar{\varepsilon}_{\mathbf{q}}/2)\,. \tag{2.13}$$

T_c for the d-wave pairing is

$$\frac{4}{\tfrac{3}{2}J-W}=\frac{1}{N}\sum_{\mathbf{q}}\eta_{\mathbf{q}}^{2}F_{\mathbf{q}}(T_c)\,. \tag{2.14}$$

$E_{\mathbf{q}}$ is the quasiparticle energy, $\varepsilon_{\mathbf{q}}$ is the band energy of noninteracting electrons, $J_{\mathbf{q}}$, $W_{\mathbf{q}}$, and $K_{\mathbf{q}}$ are the Fourier transforms of J_{ij}, W_{ij}, and K_{ij}, respectively. For nearest-neighbor hopping $\varepsilon_{\mathbf{q}}=-t\gamma_{\mathbf{q}}$, $\gamma_{\mathbf{q}}=\sum_{\delta}\exp(-i\mathbf{q}\cdot\boldsymbol{\delta})$ with $\boldsymbol{\delta}$ being the vectors linking nearest neighbors. The Fock parameter $p=(1/N)\sum_{\mathbf{q}}\gamma_{\mathbf{q}}\langle c^{\dagger}_{\mathbf{q}\sigma}c_{\mathbf{q}\sigma}\rangle$ and the chemical potential μ satisfy the following equations:

$$p=-\frac{1}{N}\sum_{\mathbf{q}}\bar{\varepsilon}_{\mathbf{q}}\gamma_{\mathbf{q}}F_{\mathbf{q}}\,, \tag{2.6}$$

$$n-1=-\frac{2}{N}\sum_{\mathbf{q}}\bar{\varepsilon}_{\mathbf{q}}F_{\mathbf{q}}\,. \tag{2.7}$$

The pairing potential $V^{s}_{\mathbf{k},\mathbf{q}}$ takes on the separable form for the square lattice and the nearest-neighbor interactions, and Eq. (2.1) can be solved by an ansatz

$$\Delta_{\mathbf{k}}=\Delta_0+\Delta_\gamma\gamma_{\mathbf{k}}+\Delta_\eta\eta_{\mathbf{k}}\,, \tag{2.8}$$

where the particular terms refer to on-site s-wave, extended s-wave, and d-wave pairings, respectively,

$$\gamma_{\mathbf{k}}=2(\cos k_x+\cos k_y)\,,\quad \eta_{\mathbf{k}}=2(\cos k_x-\cos k_y)\,.$$

The self-consistent equations for the s-wave pairing are

$$\Delta_0=\frac{1}{N}\sum_{\mathbf{q}}(-U+K\gamma_{\mathbf{q}})\Delta_{\mathbf{q}}F_{\mathbf{q}}\,,$$

$$\Delta_\gamma=\frac{1}{N}\sum_{\mathbf{q}}[\tfrac{1}{4}(\tfrac{3}{2}J-W)\gamma_{\mathbf{q}}-K]\Delta_{\mathbf{q}}F_{\mathbf{q}}\,, \tag{2.9}$$

and for the d-wave pairing

$$\Delta_\eta=\frac{1}{N}\sum_{\mathbf{q}}\tfrac{1}{4}(\tfrac{3}{2}J-W)\eta_{\mathbf{q}}\Delta_{\mathbf{q}}F_{\mathbf{q}}\,. \tag{2.10}$$

The transition temperature for the onset of pure s-wave pairing is given by

B. Equal-spin (triplet) pairing

The gap equation is given by

$$\Delta_t(\mathbf{k})=\frac{1}{N}\sum_{\mathbf{q}}V^{t}_{\mathbf{k},\mathbf{q}}\langle c_{-\mathbf{q}\uparrow}c_{\mathbf{q}\uparrow}\rangle=\frac{1}{N}\sum_{\mathbf{q}}V^{t}_{\mathbf{k},\mathbf{q}}\Delta_t(\mathbf{q})F_{\mathbf{q}}\,, \tag{2.15}$$

with $F_{\mathbf{q}}$ given by (2.3) and

$$E_{\mathbf{q}}=\sqrt{\bar{\varepsilon}_{\mathbf{q}}^{2}+|\Delta_t(\mathbf{q})|^{2}}\,,$$

$$V^{t}_{\mathbf{k},\mathbf{q}}=\tfrac{1}{2}(W_{\mathbf{k}+\mathbf{q}}+\tfrac{1}{2}J_{\mathbf{k}+\mathbf{q}}-W_{\mathbf{k}-\mathbf{q}}-\tfrac{1}{2}J_{\mathbf{k}-\mathbf{q}})\,. \tag{2.16}$$

The equations for p and μ are given by (2.6) and (2.7) with $\Delta_{\mathbf{k}}$ replaced by $\Delta_t(\mathbf{k})$. For the $d=2$ square lattice and the nearest-neighbor interaction, after substituting

$$\Delta_t(\mathbf{q})=\Delta^{p}_{\mathbf{q}}=\Delta^{p}_{x}\sin q_x+\Delta^{p}_{y}\sin q_y\,,$$

one obtains

$$\Delta_\alpha^p = -\frac{2W+J}{N}\sum_{\mathbf{q}} \sin q_\alpha \Delta_{\mathbf{q}}^p F_{\mathbf{q}}, \quad \alpha = x,y . \tag{2.17}$$

Thus T_c for the onset of p-wave pairing is determined by

$$-\frac{1}{2W+J} = \frac{1}{N}\sum_{\mathbf{q}} \sin^2 q_x F_{\mathbf{q}}(T_c) , \tag{2.18}$$

together with Eqs. (2.6) and (2.7) in $\Delta_{\mathbf{q}}^p \to 0$ limit, and $F_{\mathbf{q}}(T_c)$ is given by Eq. (2.13).

As far as the spin-density-wave (SDW) ordering is concerned the mean-field equations have been given in Ref. 1. The main effect of antiferromagnetic exchange is to enhance U by adding factor Jz, z being the coordination number.

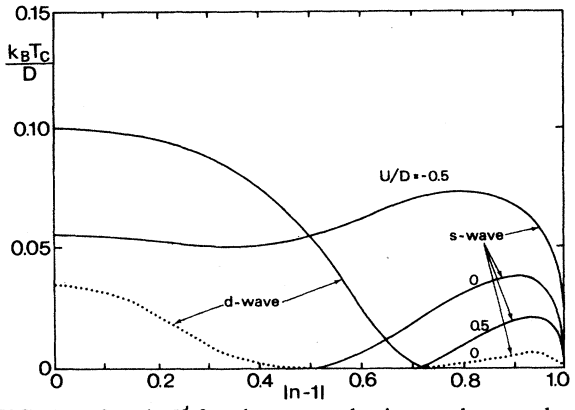

FIG. 1. T_c^s and T_c^d for the square lattice vs electron density for $J/D=1/3$ (solid lines) and for $J/D=1/6$ (dotted lines). The values U/D for T_c^s are next to corresponding curves.

III. RESULTS

The coupled equations for the superconducting transition temperatures and for the chemical potential have been solved by direct numerical integration for the square lattice (under the assumption that $p=0$). The calculations were performed for the extended range of the interaction parameters and arbitrary electron density n ($0 \le n \le 2$), including the case of nearest- and next-nearest-neighbor hopping.

A. The case of nearest-neighbor hopping

For the sake of clarity we will present first the results concerning the limiting case $W=0$, $K=0$, i.e., the case for which the intersite pairing is exclusively produced by an effective magnetic interaction.

If $n=1$, $\bar{\mu}=0$ the equations determining T_c for s,d,p pairings and SDW ordering can be analyzed by low-temperature (weak-coupling) and high-temperature expansions. There are two branches of s-type solutions for T_c which are decoupled if $n=1$ and $K=0$: (i) extended s-pairing ($\Delta_\gamma \neq 0$, $\Delta_0=0$) existing only for $J/D \ge \pi^2/12$ (U arbitrary); (ii) on-site-s-pairing ($\Delta_0 \neq 0$, $\Delta_\gamma=0$) existing for any J and $U<0$. The d-wave pairing solutions exist for arbitrary $J>0$ and $T_c^d > T_c^s$ for any $J>0$, $U>0$. In the case of a ferromagnetic exchange interaction the only possible superconducting solutions are the p pairing, existing for arbitrary U and $J<0$, and the on-site s-wave pairing.

The numerical solutions for T_c of s- and d-wave pairing for the case of $J>0$ are simply given by Fig. 1 of Ref. 1 with $|W| \to \frac{3}{2}J$, and T_c for SDW is the same as in Fig. 1 of Ref. 1 but with $U/D \to (U+4J)/D$. By comparison of critical temperatures one obtains that as far as the mutual stability of pure phases is concerned, the SDW is most stable for any $U>0$, $J>0$ and the boundary between on-site s pairing and the SDW for $J>0$ is given by $-U=2J$.

For $n \neq 1$ the nature of the ordered state depends on band filling and the values of parameters involved. In Fig. 1 we give T_c for s- and d-wave pairing for different values of J/D and U/D. These plots are symmetric with respect to $n \to 2-n$ due to the electron-hole symmetry. T_c^d is the highest one close to the half-filled band and enhanced due to the Van Hove's singularity, while T_c^s for extended s-wave pairing shows strongly nonmonotonous behavior with a sharp increase for small values of n, going through the maximum upon increasing n and dropping to zero asymptotically above some value of n. The increasing on-site repulsion U reduces T_c^s and the maximum of T_c^s is shifted towards higher values of $|n-1|$.

Such a behavior of T_c^s is obtained for any $U>0$ as long as $J < J_{\text{crit}} = (\pi^2/12)D$. For $J > J_{\text{crit}}$, T_c^s tends to finite value for $n=1$. Moreover if U is negative, the s-wave pairing can always be made the most stable one for sufficiently large values of $|U|$.

From comparison of T_c of different pairings we give the diagram of relative stability of s and d pairings in Fig. 2. The boundary between the d and s pairing states is located

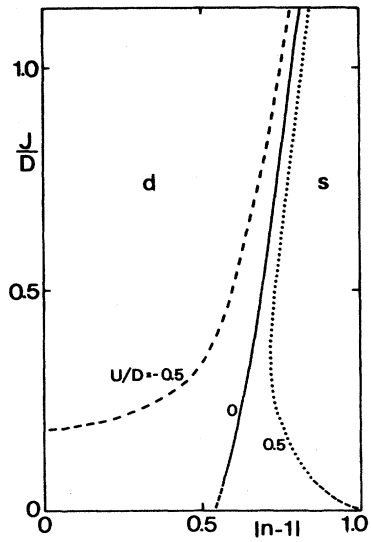

FIG. 2. Diagram for relative stability of s- and d-wave pairings for the square lattice in J/D vs $|n-1|$ plane, for $W=K=0$. The solid line is for $U=0$, the dashed line is for $U/D=-0.5$, and the dotted line is for $U/D=0.5$. The solid and dotted lines are extrapolated down to $J/D=0$, which is shown by the dashed parts.

at $0.15 < n_c < 0.46$ for $0 < J/D \leq 4/3$, $U=0$; and n_c decreases with increasing J. Increasing $U>0$ shifts n_c towards lower values, whereas $U<0$ can expand the stability region of s pairing up to $n=1$.

In Fig. 3, we present the diagram of relative stability of s-, p-, and d-wave pairings obtained for the case $J=0$ and $W<0$ (see also Ref. 1). Contrary to the case $J>0$, $W=0$, where p-wave pairing cannot exist and one expects only the $d \rightarrow s$-wave transition with decreasing n, in the case of attractive W the p-wave pairing can be most stable in the region of intermediate densities and the sequence of transitions $d \rightarrow p \rightarrow s$ is possible with lowering the electron density for $U>0$ or small negative U. Increasing the coupling constant expands the range of stability of d-wave pairings towards higher values of $|n-1|$ in both cases considered (compare Figs. 2 and 3).

Let us point out now the effects of *repulsive* intersite Coulomb interaction $W>0$. Increasing $W>0$ reduces T_c^s and T_c^d due to renormalization of the coupling constant $J \rightarrow J - \frac{2}{3}W$ and shifts the boundary between d and s pairing towards lower values of $|n-1|$.

For $W > \frac{2}{3}J$ both types of intersite pairing are suppressed for arbitrary n and only the s-wave pairing stabilized by $U<0$ can be eventually developed in the system. The other possibility for $W>0$ is stabilization of the charge-density-waves (CDW) ordering.[16,17] The Hartree-Fock analysis indicates that CDW can be established for $d=2$ if $U+4J<4W$ close to the half-filled band, whereas for $U+4J>4W$ CDW is suppressed by the SDW ordering. The coexistence of CDW and anisotropic s- and d-wave pairing is an open problem. We should mention, however, that for the $U<0$ case the coexistence of CDW and on-site s-wave pairing has been already analyzed.[16] It has been found that such a mixed phase (CDW with singlet on-site superconductivity) can be stable in a quite extended range of electron densities (except for low-density limit and $n=1$).

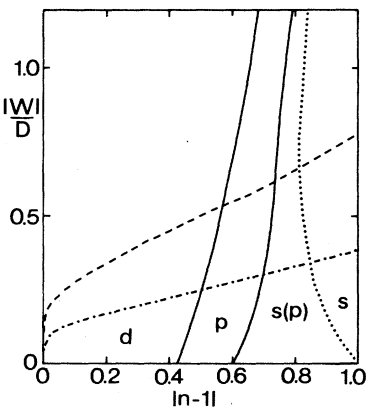

FIG. 3. Diagram of relative stability of s-, p-, and d-wave pairings for the square lattice in W/D vs $|n-1|$ plane for $J=0$, $K=0$. The p-s boundary is plotted for $U=0$ (solid line) and $U/D=0.5$ (dotted line). The dashed-dotted and the dashed lines denote the phase boundary between the superconducting and condensed phases for $U=W_{LR}=0$ and $|W|/D=U/4D + W_{LR}/2D$, respectively, with the condensed phase being stable above these border lines (see Sec. IV).

B. Effects of next-nearest-neighbor hopping

For the square lattice and next-nearest-neighbor hopping $\varepsilon_{\mathbf{k}} = -2t(\cos k_x + \cos k_y) - 4t_2 \cos k_x \cos k_y$. The t_2 term breaks the electron-hole symmetry and consequently Van Hove's singularity moves to $n \neq 1$, shifting the maximum of T_c for d- and p-wave pairing.

The results of numerical analysis of T_c vs n for s- and d-wave pairings are shown in Figs. 4(a) and 4(b) for a fixed value $J/D=1/3$ and several values of t_2/t. The cases of $t_2>0$ and $t_2<0$ are linked by the relation $T_c(n,t_2/t) = T_c(2-n,-t_2/t)$ and it is sufficient to consider only the case $t_2>0$. It is clear from Figs. 4(a) and 4(b) that for a definite range of n, T_c can be essentially altered even for small t_2. Upon increasing t_2/t the maximum of T_c^d [Fig. 4(a)] decreases and moves from $n=1$ towards higher densities and the strong nonmonotonous variation of T_c^d vs n is observed for larger t_2/t ratio.

Concerning the s-wave pairing [Fig. 4(b)] we observe that this type of pairing is enhanced in the regime $1<n<2$ and is spread over a wider range of densities. The maximum of T_c^s moves towards the half-filled band. For $0<n<1$, T_c^s is strongly suppressed upon increasing t_2 but s-wave pairing can still be stable for small n.

In Fig. 5 we compare T_c^d and T_c^s vs n for $t_2/t=0.5$ with that for $t_2=0$. In this figure we also show the effect of $U>0$ on the s-wave pairing, which results in a reduction

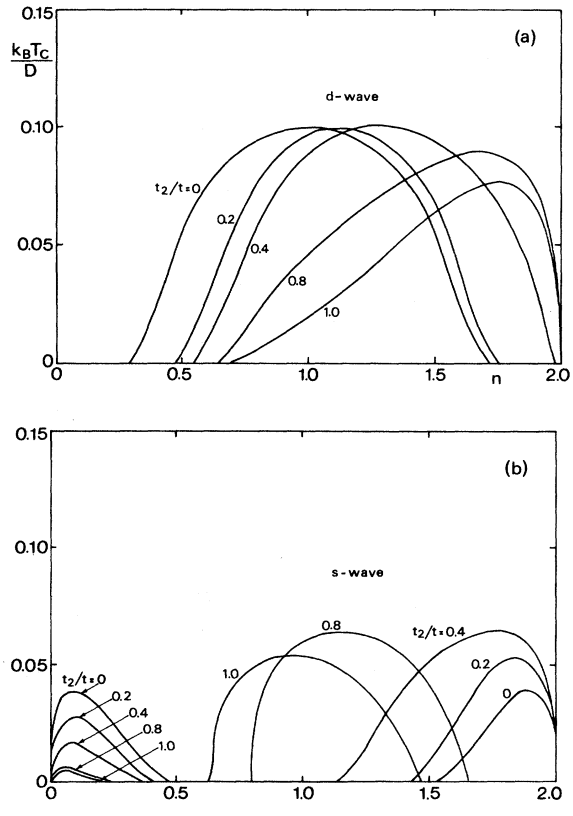

FIG. 4. T_c vs electron density for (a) d-wave pairing and for (b) s-wave pairing for different ratios of t_2/t and $J/D=1/3$ ($U=0$ for the s-wave pairing.) $d=2$ square lattice.

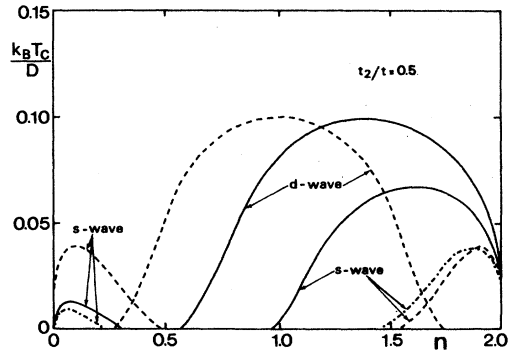

FIG. 5. Comparison of critical temperatures for d- and s-wave pairing vs n for $J/D=1/3$. The solid lines and dashed lines are for $t_2/t=0.5$ and $t_2=0$, respectively, and $U=0$ for s-wave pairing. The dashed-dotted line denotes T_c^s for $U/D=0.5$, $t_2/t=0.5$. $d=2$ square lattice.

of T_c^s and moving the maximum of T_c^s towards lower densities.

The diagram of relative stability of s- and d-wave pairings as a function of t_2/t is given in Fig. 6. To stress the reflection symmetry both cases $t_2>0$ and $t_2<0$ are presented. We notice that with increasing $t_2/t>0$ the range of stability of d-wave pairing extends up to $n=2$, while the d-s phase boundary for small n is only weakly dependent on the t_2/t ratio. Also, for large t_2/t the s-wave pairing with strongly enhanced T_c can be stabilized close to the half-filled band. Thus, with increasing t_2/t ratio the sequence of transitions as a function of n can be changed from $s\rightarrow d\rightarrow s$ to $s\rightarrow d$ and then to $s\rightarrow d\rightarrow s\rightarrow d$ (compare with Fig. 10 in Ref. 1).

C. Effects of the correlated hopping term

Let us now consider the effects of the correlated hopping term K on the superconducting transition temperatures. As it follows from the self-consistent equations for the d-wave and p-wave pairing the K coupling enters them only in the form of normal Hartree-Fock terms [compare Eqs. (2.6) and (2.7), Eq. (2.14), and Eq. (2.18)].

Thus its effect reduces to some (unessential) renormalization of the bandwidth and the chemical potential, which can be neglected in the first approximation.

In the case of s-wave pairing the effect of K term is much more essential as it enters explicitly the corresponding pairing potential.

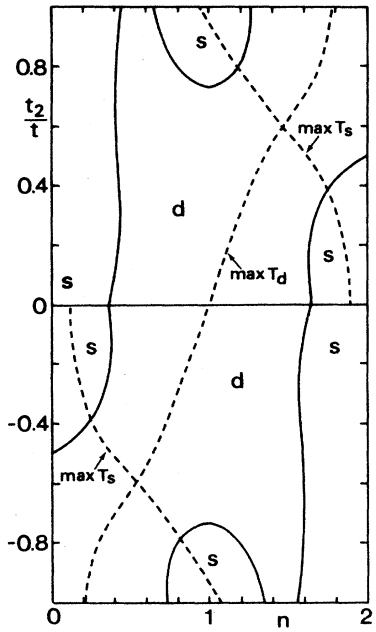

FIG. 6. Diagram for relative stability of s- and d-wave pairings in t_2/t vs n plane for $J/D=1/3$ ($U=0, W=0$). The solid lines separate the phases with s and d pairings, while the dashed lines mark the maxima for T_c^s and T_c^d.

It is instructive to consider first the case of rectangular density of states of the form $\rho(\varepsilon)=(1/2D)\Theta(D-|\varepsilon|)$ where $\Theta(x)$ is the Heaviside function and D is the half bandwidth. Upon using the weak-coupling approximation one obtains for Φ_1, Φ_2, and Φ_γ (neglecting the normal Hartree-Fock terms):

$$\Phi_1=\frac{1}{2D}Y, \tag{3.1a}$$

$$\Phi_2=\frac{n-1}{2t}-\frac{\bar{\mu}}{2tD}Y, \tag{3.1b}$$

$$\Phi_\gamma=\frac{1}{4t^2D}[D^2+\bar{\mu}^2-4D\bar{\mu}(n-1)+2\bar{\mu}^2Y], \tag{3.1c}$$

where

$$Y=\ln\left(\frac{\sqrt{D^2-\bar{\mu}^2}}{k_BT_c}\frac{2e^C}{\pi}\right). \tag{3.1d}$$

$C=0.577$ is the Euler constant and, at $T=0$ K, $\bar{\mu}=D(n-1)$. Equations (2.11) and (3.1a)-(3.1d) yield the following expression for T_c of s-wave pairing:

$$\frac{k_BT_c}{D}=1.13\sqrt{n(2-n)}\exp\left(-\frac{2[1+\tilde{K}(n-1)]^2-\lambda[1-3(n-1)^2]+2\lambda u(n-1)^2}{2\lambda(n-1)^2+(\lambda u+\tilde{K}^2)[1+(n-1)^2]+4\tilde{K}(n-1)-2u}\right), \tag{3.2}$$

where $\tilde{K}=K/2t$, $u=U/2D$, $\lambda=(\frac{3}{2}J-W)/2t$, $D=4t$. T_c^s given by (3.2) shows nonmonotonic behavior with n and a maximum of T_c^s occurs for $n\neq 1$.

For the two-dimensional square lattice, the T_c^s has been determined numerically from Eqs. (2.11) and (2.7) and the results are shown in Figs. 7 and 8. Figure 7 shows T_c^s vs n for a given ratio $(W-\frac{3}{2}J)/D=-0.5$ and different values of K/D. Upon increasing K/D ($K>0$), T_c^s is substantially enhanced in the regime $1<n<2$ and s-wave pairing extends over a wider range of densities. For $0<n<1$, T_c^s is reduced and the s-p (d) phase boundary is shifted toward smaller densities.

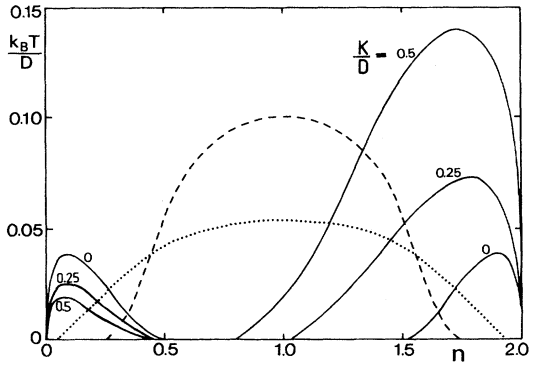

FIG. 7. T_c^s vs electron density for fixed value of $(W-\frac{3}{2}J)/D=-0.5$, $U=0$, and different values of the correlated hopping K/D given next to the solid curves. For comparison T_c^d and T_c^p for $W/D=-0.5$, $J=0$ is plotted by the dashed and dotted lines, respectively. $d=2$ square lattice.

We should point out that the K term breaks the electron-hole symmetry and similarly as in the case of the next-nearest-neighbor hopping there exists the following relation for T_c^s: $T_c^s(n,K,\dots)=T_c^s(2-n,-K,\dots)$, which links the cases of $K>0$ and $K<0$, respectively (provided that Hartree-Fock terms in $\bar{\varepsilon}_q$ are neglected). In Fig. 8 T_c^s vs n is plotted for the case $W=J=0$ and different values of K/D and U/D. This figure shows that there is a potential possibility of having the s-wave pairing due to the K term only, i.e., even if all the other mechanisms of pairing (i.e., $W<0$, J, or $U<0$) are absent.

However, as the pairing induced by this term always consists of on-site s-wave and the extended s-wave components ($\Delta_0\neq 0$, $\Delta_\gamma\neq 0$), it will be strongly suppressed by both the on-site repulsion $U>0$ and the intersite repulsion $W>0$. Thus except for very special cases the correlated hopping term alone cannot serve as a driving mechanism of superconducting pairing. In particular, it becomes completely uneffective in the large-U limit.

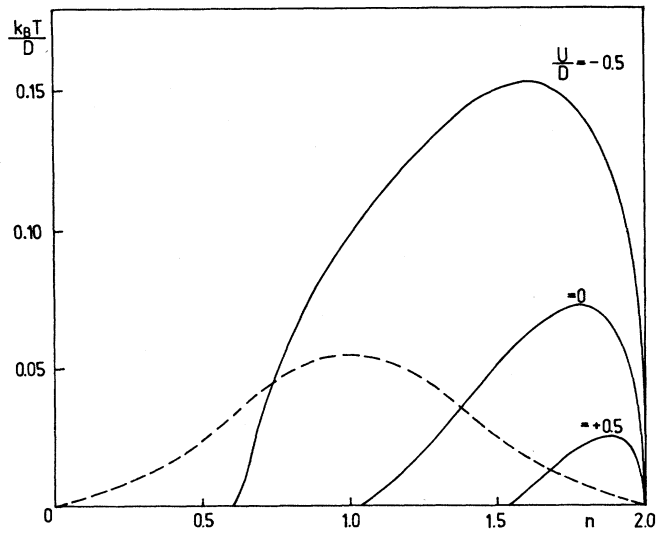

FIG. 8. T_c^s vs electron density for $K/D=0.5$ ($W=J=0$) and different values of U/D, for the square lattice and nearest-neighbor hopping. The dashed line denotes T_c^s for $U/D=-0.5$, $K=0$.

It should be stressed, however, that in the presence of other terms favoring superconductivity the effects of K can be important, and they can substantially modify the relative stability of superconducting states and the variation of T_c with the electron concentration.

IV. CONDENSATION TRANSITION

In the presence of an attractive density-density interaction the electronic system can undergo under definite conditions a condensation phase separation transition, such as liquid-gas condensation. For the case of the half-filled band, this problem has been recently discussed by Gubernatis *et al.*[18] for the two-dimensional spinless fermion model and by Lin and Hirsch[19] for the one-dimensional extended Hubbard model with nearest-neighbor interaction. In particular, for the latter model it was found by the combination of the analytic results and the Monte Carlo simulations that the condensed phase occupies an essential part of the U,W plane of the ground-state phase diagram for $W<0$.

Let us first consider some particular limits of the Hamiltonian (1.1) for the case of attractive interaction, for which one can find the relation with appropriate pseudospin models.

(i) In $t=0$ limit, upon substitution $S_i=n_{i\uparrow}+n_{i\downarrow}-1$ the Hamiltonian (1.1) can be transformed into[20]

$$H=N(\tfrac{1}{2}zW-U)-(\mu-zW-\tfrac{1}{2}U)\sum_i S_i+\tfrac{1}{2}U\sum_i S_i^2+\tfrac{1}{2}\sum_{i,j}W_{ij}S_iS_j\,, \tag{4.1}$$

together with the condition

$$\frac{1}{N}\sum_i\langle S_i\rangle=n-1\,. \tag{4.2}$$

Therefore the system is equivalent to the $S=1$ Ising model with single-ion anisotropy and with the eigenvalue zero doubly degenerate in an effective magnetic field given self-consistently by (4.2). For the half-filled band $\mu=zW+\frac{1}{2}U$ and the thermodynamic properties of (4.1) are the same as those of the Blume-Capel model with the anisotropy parameter $D=U/2+k_BT\ln 2$.[20] For $W<0$ the ferromagnetic order of pseudospins will correspond to electron droplet formation. In the ground state for $U>0$ the transition between the droplet phase and the Mott phase (i.e., the phase with one electron per site configuration) is of first order and takes place for $U/z|W|=\frac{1}{2}$ (exact result). For finite temperatures the transition can be of first or second order together with the tricritical point. For $U<0$, $W<0$ the droplet phase (ferromagnetic order) is always stable at $T=0$ and a transition to the disordered phase at finite room temperature is of second order.

On the other hand for $W>0$ the charge-order (antiferromagnetism of pseudospins) can develop[20] and at $T=0$ K it is a stable phase for any $zW>2U$.

For the non-half-filled band, the analysis of (1.1) in the $t=0$ limit or (4.1) has also been performed but only for $W>0$ (Ref. 20) and the problem of droplet formation for $W<0$, $n\neq 1$ has not been studied so far.

(ii) For $U<0$ and $|U|\gg t, W$ the perturbation theory can be used to derive an effective pseudospin Hamiltonian of the form[16]

$$\mathcal{H}=-\tfrac{1}{2}\sum_{i,j}\bar{J}_{ij}(\rho_i^{+}\rho_j^{-}+\rho_i^{-}\rho_j^{+})+\sum_{i,j}\bar{K}_{ij}\rho_i^{z}\rho_j^{z}-B\sum_i(2\rho_i^{z}+1)-\tfrac{1}{4}N(\bar{J}_0+2W_0)\,, \tag{4.3}$$

together with the condition

$$\frac{1}{N}\sum_i\langle 2\rho_i^{z}+1\rangle=n\,, \tag{4.4}$$

where

$$\bar{J}_{ij}=2t_{ij}^2/|U|,\quad \bar{K}_{ij}=\bar{J}_{ij}+2W_{ij},\quad B=\mu+\tfrac{1}{2}|U|-W_0\,,$$
$$\bar{J}_0=\sum_j\bar{J}_{ij},\quad W_0=\sum_j W_{ij}\,.$$

The charge operators

$$\rho_i^{+}=c_{i\uparrow}^{\dagger}c_{i\downarrow}^{\dagger},\quad \rho_i^{-}=(\rho_i^{+})^{\dagger},\quad \rho_i^{z}=\tfrac{1}{2}(n_{i\uparrow}+n_{i\downarrow}-1)$$

have $s=\frac{1}{2}$ Pauli statistics. This is the anisotropic Heisenberg antiferromagnet in an effective magnetic field, which again has to be determined self-consistently by Eq. (4.4). It has been demonstrated by the spin-wave method[21] that the superconducting ground state of (4.3) and (4.4) becomes unstable towards droplet formation for $\bar{K}/\bar{J}\leq -1$ (i.e., $-W\leq\bar{J}$) and any n. Apart from these two cases not much is known about the condensation transition for the extended Hubbard model with arbitrary electron density.

In the following we will present the results concerning the condensation transition for the two-dimensional extended Hubbard model [Eq. (1.1)] including in addition explicitly the long-range part of Coulomb interaction. Moreover, contrary to Refs. 18 and 19, the case of arbitrary electron concentration has been analyzed. In order to determine the condensation transition we consider the zero-frequency $\mathbf{q}$-dependent density-density susceptibility

$$\Pi(\mathbf{q})=\int_0^{\beta}\langle\rho_{\mathbf{q}}(\tau)\rho_{\mathbf{q}}^{\dagger}(0)\rangle d\tau\,, \tag{4.5}$$

where

$$\rho_{\mathbf{q}}=\sum_{\mathbf{k}\sigma}c_{\mathbf{k}+\mathbf{q},\sigma}^{\dagger}c_{\mathbf{k}\sigma} \tag{4.6}$$

is the density operator. Within the RPA one gets for $\Pi(\mathbf{q})$,

$$\Pi_{\mathrm{RPA}}(\mathbf{q})=\frac{\Pi_0(\mathbf{q})}{1+G_{\mathbf{q}}\Pi_0(\mathbf{q})}\,, \tag{4.7}$$

where

$$\Pi_0(\mathbf{q})=\frac{1}{N}\sum_{\mathbf{k}}\frac{f(\bar{\varepsilon}_{\mathbf{k}+\mathbf{q}})-f(\bar{\varepsilon}_{\mathbf{k}})}{\bar{\varepsilon}_{\mathbf{q}}-\bar{\varepsilon}_{\mathbf{k}+\mathbf{q}}} \tag{4.8}$$

is the noninteracting particle-hole bubble:

$$G_{\mathbf{q}}=U+2W_{\mathbf{q}},\quad \bar{\varepsilon}_{\mathbf{k}}=\varepsilon_{\mathbf{k}}-\bar{\mu},\quad \bar{\mu}=\mu-n(\tfrac{1}{2}U+W_0)\,,$$

$f(\bar{\varepsilon}_{\mathbf{k}})$ being the Fermi-Dirac distribution function. The condensation instability temperature T_{con} determined as the temperature at which $\Pi_{\mathrm{RPA}}(0)$ diverges is given by the following equations:

$$1+G_0\Pi_0(0)=0\,, \tag{4.9}$$

$$\Pi_0(0)=\frac{1}{4N}\sum_{\mathbf{k}}\frac{\beta_c}{\cosh^2(\beta_c\bar{\varepsilon}_{\mathbf{k}}/2)}\,, \tag{4.10}$$

where

$$G_0=U+2\sum_n z_nW_n=U-8|W|+2W_{\mathrm{LR}}$$

in $d=2$ and $W_{\mathrm{LR}}=\sum_{n\geq 2}z_nW_n$ denotes the long-range part of the Coulomb interaction. Equations (4.9) and (4.10) should then be solved together with the equation determining the chemical potential, i.e.,

$$n-1=-\frac{1}{N}\sum_{\mathbf{k}}\tanh\left(\frac{\beta_c\bar{\varepsilon}_{\mathbf{k}}}{2}\right). \tag{4.11}$$

This set of equations determining T_{con} has been analyzed numerically for the $d=2$ square lattice and also for the case of rectangular density of states (DOS). The critical values of $G/D=-G_0/4D=2|W|/D-U/4D-W_{\mathrm{LR}}/2D$ above which the condensation transition can occur at $T=0$ K are given as a function of electron density in Fig. 9(a).

The case of half-filled band for square lattice is very peculiar as it is the only case for which the condensation can develop for any $G>0$. This is due to the presence of the Van Hove singularity coinciding with the Fermi level. In contrast to the rectangular DOS, as well as for any $d=3$ DOS, the condensation transition is possible only above some finite value of G/D [for example, for elliptic DOS $(G/D)_{\mathrm{crit}}=4/\pi$].

For $n=1$, $\bar{\mu}=0$, and the low- and high-temperature expansions of Eqs. (4.9) and (4.10) yield for $d=2$ lattice:

$$k_BT_{\mathrm{con}}=4\exp\left(-\frac{\pi^2D}{4G}\right)\quad\text{for } 0<G\ll D\,,$$
$$k_BT_{\mathrm{con}}=G\left(1-\frac{t^2}{G^2}\right)\quad\text{for } G\gg D\,, \tag{4.12}$$

whereas for the rectangular DOS T_{con} is given by

$$k_BT_{\mathrm{con}}=\frac{D}{2}\left[\operatorname{arctanh}\left(\frac{2G}{D}\right)\right]^{-1}. \tag{4.13}$$

The numerical plots of T_{con} vs G/D for $n=1$ are given in Fig. 9(b). As is seen from Fig. 9(a) for the $d=2$ lattice even a small deviation from $n=1$ makes the condensation much less favorable to occur and yields a sharp increase of G_{crit}. Moreover for $G/D<0.7846$ there always exists a critical concentration n_c below which the condensation can never occur. This is clearly seen from Fig. 10, where the numerical plots of T_{con} vs n are given for several fixed values of G/D. A comparison of condensation transition temperature and the superconducting transition temperatures versus electron density yields the mutual stability phase diagram given in Fig. 3. This diagram includes an extreme case $U=0$, $W_{\mathrm{LR}}=0$, and also shows rapid shift of

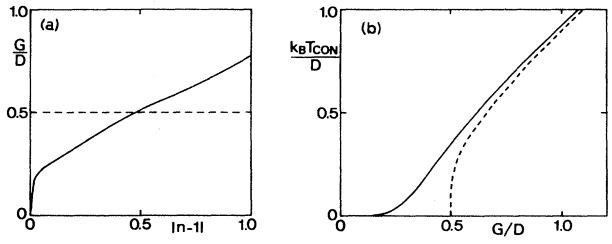

FIG. 9. (a) G/D vs $|n-1|$ diagram for condensation instability at $T=0$ for the square lattice ($G/D=2|W|/D-U/4D-W_{LR}/2D$). The dashed line denotes the condensation instability for the rectangular DOS. $t_2=0$. (b) T_{con} vs G/D for $n=1$. The solid and dashed lines are for the $d=2$ DOS and the rectangular DOS, respectively.

the phase separation line towards higher values of $|W|/D$ upon increasing of the repulsive Coulomb interactions.

We have analyzed also the influence of next-nearest-neighbor hopping on T_{con}. As in the case of the superconducting pairings T_{con} for $t_2>0$ and $t_2<0$ is linked by the relation

$$T_{con}(n,t_2/t)=T_{con}(2-n,-t_2/t)\,.$$

Upon increasing t_2/t ($t_2>0$) the maximum of T_{con} moves towards higher densities and nonzero T_{con} spreads over a wider range of densities in the regime $1<n<2$. In the regime $0<n<1$, T_{con} is strongly reduced and n_c for the onset of condensation at the ground state is shifted towards higher densities. In Fig. 10, T_{con} vs n for $G/D=0.5$ and $t_2/t=0.3$ is plotted by a dashed line.

V. FINAL REMARKS

In this paper we presented further mean-field studies of anisotropic superconductivity and condensation transition in the two-dimensional extended Hubbard model. These results were mainly oriented to show the effects of direct exchange interaction and the correlated hopping term on the stabilization of various superconducting pairings versus the band filling for $d=2$ square lattice. We have also discussed the condensation transition for the extended Hubbard model with attractive intersite interaction and arbitrary electron density. We presented the results for the pure phases only, leaving the discussion of the coexisting SDW with superconductivity and the mixed superconducting solutions to another work.

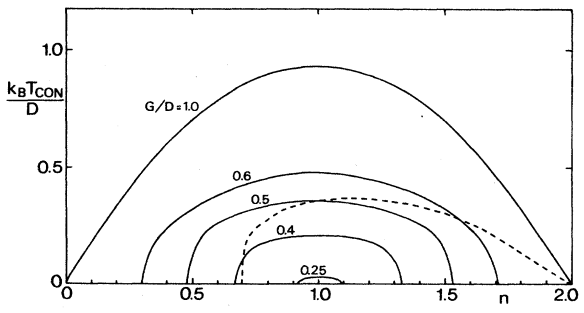

FIG. 10. T_{con} vs electron density for different values of G/D and nearest-neighbor hopping for the square lattice (solid lines). The dashed line denotes T_{con} for $G/D=0.5$ and $t_2/t=0.3$.

It is worthwhile to compare the superconducting phases with intersite pairing stabilized by intersite terms ($W<0,J$) with the superconducting on-site pairing of the attractive Hubbard model.

If $W=0$ T_c for *on-site pairing* (which is isotropic s wave) shows monotonic behaviors versus electron density with a maximum at $n=1$ and for the square lattice it is strongly enhanced by the Van Hove singularity.[1] For $d=2$ this pairing can exist for any $U<0$ and arbitrary n. If $W>0$, T_c becomes nonmonotonic[16] with a maximum of T_c at the border with CDW and above some critical density the superconductivity can coexist with CDW.

On the other hand the *intersite pairing* can be of anisotropic s-, d-, or p-wave type depending on the symmetry of pairing potential, the strength of interaction parameters, the electron density, and t_2/t ratio. All these pairings can be driven by the intersite density-density attraction $W<0$, whereas the antiferromagnetic exchange enhances extended s and d pairing and suppresses p pairing.

T_c vs n for extended s pairing is strongly nonmonotonous with a maximum for low densities (if $t_2=0$), whereas the maximum of T_c^d occurs at the border with SDW close to the half-filled band. Further differences are related with the tendency towards droplet formation and phase separation. For example, for $U<0$, $W=0$ the system never undergoes condensation while for $W<0$ this tendency is quite substantial to such an extent that for $n\approx 1$ additional repulsive Coulomb interactions (long-ranged or on-site) are necessary to stabilize superconductivity. As it was previously stressed[1] for the on-site attraction ($U<0$) one can go continuously to the large attraction limit, i.e., from the Cooper pairs to the local pairs,[16,22] at least at $T=0$ K, and there exists an exact mapping of the $U<0$ extended Hubbard model onto the hard-core charged Bose gas on a lattice for $|U|\gg t,W,k_BT$.[16]

It is an interesting problem concerning the formation of real-intersite pairs and the transition from the BCS superconductivity to superfluidity of charged bosons in the case of intersite pairing. We should mention that for the continuum case such a changeover exists and is smooth as it has been proven by Nozieres and Schmitt-Rink.[22] So far for the fermions on a lattice this is an open problem. However, recent calculations of the binding energy of a single intersite pair support such a possibility.[23]

In our previous papers,[1,24] we have already pointed out a possible relevance of the intersite pairing for the high-T_c superconducting oxides and shortly discussed the various hypotheses regarding the possible types of pairing in these materials.

The concept which seems to be well substantiated at present is that upon doping the extra holes go to the oxygen ions. Hence, the pairing occurs primarily on (neighboring) oxygen ions, i.e., we deal with the case of intersite pairing of holes on oxygen (p^5-p^5).[25] Such a picture is

strongly supported by recent spectroscopic data which identify the charge carriers in the normal state as the holes in the oxygen p band, as well as by possible peroxide (or superoxide) formation.[26-29] Moreover, recent theoretical studies support the existence of an effective (short-range) attraction just between the p holes on oxygens, induced either by (i) coupling to local magnetic configuration of Cu^{2+},[25] (ii) polarization mechanism,[30] (iii) electronic correlations,[25,31,32] particularly due to Cu-O repulsion.[31]

In contrast to the hypothesis of pairing d holes on Cu sites which would correspond to the nearly half-filled band case, now we approach the model (1.1) from the opposite side of electron densities, namely from the limit of small concentrations of holes in the p-like band (i.e., for example La_2CuO_4, with Cu^{2+} ions, will correspond to $n=0$ in the p-holes representation). In such a case theory predicts s-wave-type pairing which is isotropic, for $U<0$, and anisotropic-extended s for $W<0$ or $J\neq 0$. T_c vs n is nonmonotonic and has a maximum for some n. In fact the $n(x)$ dependence of T_c recently observed in $La_{2-x}Sr_xCuO_4$,[33] is very similar to the plots of T_c^s vs n given in Figs. 3–6 of Ref. 1 or in Figs. 1, 4(b), 5, 7, and 8 of this paper.

The model considered seems to account also for several other experimental findings:

(i) T_c and Δ can be high and n dependent since pairing takes place in the whole Brillouin zone, contrary to the BCS model.

(ii) The short coherence length observed in these materials is consistent with the model assuming local, short-range interactions.

(iii) The linear in T behavior of the resistivity in the a-b plane can be accounted for by low-carrier p-holes concentration, reinforced by quasi-two-dimensional transport.[34] As we have shown in Sec. II and in a previous paper,[1] in the case of intersite pairing there can be a transition from extended s-wave to d-wave (or p-wave) state upon increasing n. Eventual observation of such a behavior would provide further support in favor of intersite pairing and exclude the concept of on-site pairing. This is a possibility for the higher T_c materials based on Bi and Tl and having higher n.

Let us stress that our conclusions have been mostly derived on the basis of the broken-symmetry Hartree-Fock approach, which is perhaps better justified for p-like electrons than for strongly correlated d electrons. However, even for p electrons the nature of the many-body state in the presence of local attraction can depend on the density of carriers and in the small density limit the formation of real bound pairs is likely to occur. Moreover, low dimensionality of lattice structure provides an additional factor in favor of it, as in two dimensions even weak attraction can produce a bound state of two holes.[23] In such a case the superconductivity will result from the Bose condensation of these pairs and their superfluidity. Increasing carrier concentration can yield a changeover to the weak-coupling behavior.

In summary, we have presented further results concerning the superconductivity with intersite electron pairing and the electron-droplet formation in narrow band for two dimensions, which completes our previous mean-field studies.[1] We think that the results of the present paper can be also relevant to heavy-fermion superconductivity[9,10,35,36] as well as to the organic charge transfer salts, both $(TMTSF)_2X$ family and BEDT-TTF salts.[37,38]

Note added in proof: Recently, J. E. Hirsch [Phys. Lett. A **136**, 163 (1989)] has pointed out that the correlated hopping term K can arise for hole conduction through oxygen ions when coupling to a degree of freedom describing the deformation of the outer electron cloud of the ion by the presence of the conducting hole is included.

ACKNOWLEDGMENTS

R.M. would like to thank Centre de Recherche sur les Très Basses Températures, Centre National de la Recherche Scientifique Laboratory, Grenoble, where most of the results of this paper have been done. S.R. would like to thank Professor Ph. Nozieres and the Institute Laue-Langevin, Grenoble for their hospitality. We would also like to thank S. Tabor for his contribution to numerical work. R.M. and J.R. gratefully acknowledge their invitation to Institute of Scientific Interchange, which made possible the completion of this work. Two of us gratefully acknowledge the partial financial support from the Polish Academy of Sciences within Projects No. RPBP 01.09 (S.R. and R.M.) and No. CPBP 01.12 (R.M.).

*Permanent address: Institute of Physics, A. Mickiewicz University, 60-780 Poznań, Poland.

[1] R. Micnas, J. Ranninger, S. Robaszkiewicz, and S. Tabor, Phys. Rev. B **37**, 9410 (1988); see also R. Micnas, J. Ranninger, and S. Robaszkiewicz, J. Phys. C **21**, L145 (1988).

[2] J. Hubbard, Proc. R. Soc. London, Ser. A **276**, 238 (1963).

[3] L. G. Caron and G. W. Pratt, Rev. Mod. Phys. **40**, 802 (1968).

[4] S. Kivelson, W. P. Su. J. R. Schrieffer, and A. J. Heeger, Phys. Rev. Lett. **58**, 1899 (1987); **60**, 72 (1988).

[5] D. Baeriswyl, P. Horsch, and K. Maki, Phys. Rev. Lett. **60**, 70 (1988).

[6] J. Tinka Gammel and D. K. Campbell, Phys. Rev. Lett. **60**, 71 (1988).

[7] D. K. Campbell, J. Tinka Gammel, and E. Y. Loh, Jr., Phys. Rev. B **38**, 12043 (1988).

[8] P. W. Anderson, in *Solid State Physics,* edited by F. Seitz and D. Turnbull (Academic, New York, 1963), Vol. 14, p. 99.

[9] K. Miyake, T. Matsuura, H. Jichu, and Y. Nagaoka, Prog. Theor. Phys. **72**, 1063 (1984).

[10] F. J. Ohkawa and H. Fukuyama, J. Phys. Soc. Jpn. **53**, 4344 (1984).

[11] J. E. Hirsch, Phys. Rev. B **35**, 8726 (1987).

[12] F. J. Ohkawa, Jpn. J. Appl. Phys. **26**, L652 (1987); J. Phys. Soc. Jpn. **56**, 2267 (1987).

[13] H. Shimahara and S. Takada, Jpn. J. Appl. Phys. **26**, L1674 (1987).

[14] Y. Kuramoto and T. Watanabe, Solid State Commun. **63**, 821 (1987).

[15] Wei-ming Que and G. Kirczenov, Solid State Commun. **64**, 1053 (1987).

[16]S. Robaszkiewicz, R. Micnas, and K. A. Chao, Phys. Rev. B **23**, 1447 (1981); **24**, 1579 (1981); **24**, 4018 (1981); **26**, 3915 (1982).
[17]J. Zhong, K. Zhang, K. A. Chao, R. Micnas, and S. Robaszkiewicz, Phys. Status Solidi (b) **133**, 143 (1986).
[18]J. E. Gubernatis, D. J. Scalapino, R. L. Sugar, and W. D. Toussaint, Phys. Rev. B **32**, 103 (1985).
[19]H. Q. Lin and J. E. Hirsch, Phys. Rev. B **33**, 8155 (1986).
[20]R. Micnas, S. Robaszkiewicz, and K. A. Chao, Phys. Rev. B **29**, 2784 (1984), and references therein.
[21]A. S. Alexandrov, J. Ranninger, and S. Robaszkiewicz, Phys. Rev. B **33**, 4526 (1986).
[22]Ph. Nozieres and S. Schmitt-Rink, J. Low Temp. Phys. **59**, 195 (1985).
[23]R. Micnas (unpublished).
[24]R. Micnas, J. Ranninger, and S. Robaszkiewicz, in *Proceedings of the International Conference on Magnetism (ICM'88), Paris, 1988* [J. Phys. (Paris), Colloq. Suppl. **49**, C8-2221 (1988)].
[25]V. J. Emery, Phys. Rev. Lett. **58**, 2794 (1987); V. J. Emery and G. Reiter, Phys. Rev. B **38**, 4547 (1988).
[26]J. M. Tranquada, S. M. Heald, and A. R. Moodenbaugh, Phys. Rev. B **36**, 5263 (1987); N. Nücker *et al.*, *ibid.* **37**, 5158 (1988).
[27]D. D. Sarma, K. Sredhar, P. Ganguly, and C. N. R. Rao, Phys. Rev. B **36**, 2371 (1987); D. D. Sarma, K. Prabhakaran, and C. N. R. Rao, Solid State Commun. **62**, 263 (1988).
[28]D. D. Sarma and C. N. R. Rao, J. Phys. C **20**, L659 (1987); Solid State Commun. **65**, 47 (1988).
[29]J. W. Rogers, Jr. *et al.*, Phys. Rev. B **38**, 5021 (1988).
[30]A. J. Fedro, H. B. Schüttler, and S. K. Sinha, Physica B **148**, 250 (1987); C. M. Varma, S. Schmitt-Rink, and E. Abrahams, Solid State Commun. **62**, 681 (1987).
[31]J. E. Hirsch *et al.*, Phys. Rev. Lett. **60**, 1668 (1988); M. D. Nunez Regueiro and A. A. Aligia, *ibid.* **61**, 1889 (1988).
[32]B. K. Chakraverty, D. D. Sarma, and C. N. R. Rao, Physica C **156**, 413 (1988).
[33]J. B. Torrrance *et al.*, Phys. Rev. Lett. **61**, 1127 (1988).
[34]R. Micnas, J. Ranninger, and S. Robaszkiewicz, Phys. Rev. B **36**, 4051 (1987); D. Y. Xing, M. Liu, and C. S. Ting, *ibid.* **37**, 9769 (1988).
[35]F. J. Ohkawa, J. Phys. Soc. Jpn. **53**, 3568 (1984).
[36]C. Bastide and C. Lacroix, Europhys. Lett. **4**, 935 (1987); C. Bastide and C. Lacroix, J. Phys. F **18**, 63 (1988); C. Bastide and C. Lacroix, J. Phys. C (to be published).
[37]T. Ishiguro, Physica **153-155**, 1955 (1988).
[38]Y. Hasegawa and H. Fukuyama, J. Phys. Soc. Jpn. **55**, 3978 (1986).